Gut-liver interaction study on an all-polydimethylsiloxane microfluidic device integrating intestinal paracellular permeability assay

Ryuya Kida, Alan Rajendran, Mamiko Tsugane, Jean-Charles Duclos-Vallée, Maxime M Mahe, Sakina Bensalem, Hiroaki Suzuki, Bruno Le Pioufle

Talanta Open 9 (2024) 100289

Contents lists available at ScienceDirect

Talanta Open

journal homepage: www.sciencedirect.com/journal/talanta-open

Gut-liver interaction study on an all-polydimethylsiloxane microfluidic device integrating intestinal paracellular permeability assay

Ryuya Kida [a], Alan Rajendran [b,c], Mamiko Tsugane [a], Jean-Charles Duclos-Vallée [c], Maxime M Mahe [d,e,f], Sakina Bensalem [b], Hiroaki Suzuki [a], Bruno Le Piouffle [b,*]

[a] Graduate school of Science and Engineering, Chuo University, Japan
[b] Université Paris Saclay, ENS Paris Saclay, CNRS, LUMIN, France
[c] Université Paris Saclay, Inserm UMR_S 1193, FHU Hepatinov, France
[d] Division of Pediatric General and Thoracic Surgery, Cincinnati Children's Hospital Medical Center, USA
[e] Center for Stem Cell and Organoid Medicine, Cincinnati Children's Hospital Medical Center, USA
[f] The Enteric Nervous System in Gut and Brain Diseases, Nantes Université, Inserm, TENS UMR1235, IMAD, France

ARTICLE INFO

Keywords:
Microphysiological system
Co-culture
Liver-gut axis
Paracellular permeability
Bile

ABSTRACT

Microphysiological systems (MPSs) have attracted increasing attention as a method for simulating in vitro drug efficiency. In particular, the interaction between liver and intestine tissues is one of the primary targets since they are closely involved in drug absorption and metabolism. However, most of the intestine-liver MPSs reported previously require pumps, electrodes, and porous membranes for co-culture of cells and evaluation of intestinal permeability (i.e., Trans-Epithelial Electrical Resistance, TEER), requiring complex manufacturing processes and operations. In this study, we report an all-polydimethylsiloxane (PDMS) co-culture microfluidic device, connecting microchamber-based paracellular transport assay on gut microtissues to liver tissues matured on the same device. On one side of the device, HepaRG cells are confined within thin parallel grooves that induce their differentiation into hepatocytes. The other side of the device is connected with microchannels to the liver side and includes the gut tissues, organized above microchambers. Such microchambers allow the evaluation of paracellular permeability by fluorescence imaging. Thanks to the microfluidic device we investigated changes in intestinal permeability induced by differentiated hepatocyte excretion and found that Caco-2 permeability was decreased when co-culture with HepaRG. Due to its simplicity and straightforward implementation, this method is anticipated as an innovative and efficient approach to assess tissue barrier function in multi-organ on-chip experiments.

1. Introduction

Recently, microphysiological Systems (MPSs), designed to replicate microenvironment of human organ functions on microchips, have garnered significant attention [1–3]. In the process of drug development, animal experiments raise ethical concerns, and discrepancies between the outcomes of these experiments and human clinical trials pose significant challenges [4–6]. Additionally, conventional two-dimensional cell cultures using dishes or flasks often fail to maintain the appropriate cellular functionality due to their significant deviation from the in vivo cellular environment and the lack of interactions between multiple cell types, frequently resulting in responses that differ markedly from human clinical outcomes [7]. In contrast, MPSs offer the ability to cultivate cells in environments that closely mimic the intricate structures of the human body. Furthermore, they allow for the replication of interactions between various cell types. As a result, MPSs hold promise not only for advancing drug development but also for personalized medicine by tailoring treatments to individual patients and for elucidating the mechanisms of diseases. Indeed, Huh et al., have developed a lung on a chip that replicates shear stress and cyclic strain, successfully reproducing complex cellular responses to bacteria and inflammatory cytokines on a chip-based platform [8]. Amidst the ongoing development of various types of MPSs such as those for the heart, blood vessels, and the blood-brain barrier [9–13], our research has focused on the intestine and liver. These two organs play pivotal roles in drug absorption and metabolism [14,15], making them essential

* Corresponding author.
E-mail address: bruno.le-pioufle@ens-paris-saclay.fr (B.L. Pioufle).

https://doi.org/10.1016/j.talo.2024.100289
Received 2 December 2023; Received in revised form 20 January 2024; Accepted 20 January 2024
Available online 21 January 2024

candidates for MPS-based investigations.

In previous studies, several attempts have been made to establish the gut-liver MPSs, in addition to the conventional Transwell-type co-culture systems [16–18] reflecting their importance. For instance, Tsamandouras et al. [19] and Yang et al. [20] separately established MPS models for simulating non-alcoholic fatty liver disease (NAFLD) on a microchip integrated with pneumatic pumps for drug testing. Similarly, Kimura's group reported the development of a microchip-based model to study the effects of anticancer drugs [21] or the fundamental interactions [22] More recently, Kang et al. [23] developed a gut-liver axis chip and tested the effect of metabolites of microbiomes and extracellular vesicles. However, it is worth noting that many of these co-culture systems have required complex setups involving pumps and tubings for precise medium perfusion, which increases the cost and level of complexity of experiments. Especially, integration of the porous membrane-based epithelial permeability assay or TEER measurements into MPSs [24,25] could be cumbersome and less reproducible. Furthermore, most of the research in this field focuses on diseases and drug response, with limited exploration into more fundamental questions concerning the interaction between several organs, such as the influence of liver metabolites on intestinal permeability.

Previously, we reported the development of a microfluidic system for culture of HepaRG, a human hepatic cell line having high similarity to human primary hepatocytes and confirmed the formation of functional bile canaliculi [26]. It has been widely recognized that bile, a key liver metabolite, plays a crucial role in modulating the barrier function of intestine [27–29] in addition to the lipid digestion and absorption. Notably, an excessive primary bile secretion is known to contribute to increased intestinal permeability and disease development. Given the recognized association between abnormal gut-liver axis interactions and diseases, investigating the intricate relationship between these organs remains an essential area of study.

In this study, we aimed to overcome these challenges by developing a simple but novel all-PDMS microfluidic device designed specifically to investigate the impact of hepatocyte metabolites on intestinal permeability. This was achieved through the co-culturing of hepatocytes (HepaRG) and intestinal cells (Caco-2) in two distinct culture compartments interconnected by flow channels. To create an in vivo-like environment for hepatocyte culture, we adopted a groove structure inspired by Delalat et al.'s previous study [30]. This microarchitecture, mimicking the sinusoidal microstructure of the liver, significantly enhanced the differentiation of HepaRG cells. To assess intestinal permeability, we implemented a unique system in which adherent cells were cultured on an array of microchambers intentionally designed to be smaller than the cells themselves [31]. After the seeded cells form a monolayer and cover the microchambers, permeation of a fluorescent marker substance was measured by examining the fluorescence intensity in microchambers. Employing this method not only streamlines the manufacturing process but also allows for the localized assessment of paracellular permeability, a task that has proven challenging with traditional methods.

In the following, we first introduce the fabrication process of the device and subsequently describe the effects of co-culturing hepatocytes with intestinal epithelial cells using this innovative platform. Lastly, we discuss the effect of the human primary bile on intestinal permeability and discuss the effect of different concentrations of bile on intestinal permeability.

2. Strategies

In the present device, HepaRG, a hepatic cell line, and Caco-2 intestinal epithelial cell line were cultured in the culture compartments next to each other (Fig. 1(a)). These compartments are connected by microchannels to allow exchange of components in the media. Here, microgrooves (40 μm depth and 20–40 μm width) were engraved on the culture surface for HepaRG. As HepaRG cells fall and proliferate in microgrooves (Fig. 1(b)), the developed cell culture exhibits a structure similar to the hepatic sinusoids and enhanced metabolic activities [26, 30]. Meanwhile, microchambers of 10 × 10 μm sides and 10 μm depth were engraved on the culture surface of Caco-2 cells for the assessment of paracellular permeability of the epithelial monolayer. Previously we showed that Caco-2 cells form a monolayer over microchambers of this size without penetrating or clogging [32] (Fig. 1(c)). In this configuration, the microchamber space stays absent of the marker molecule if the epithelial barrier is tight, while fluorescence is observed using a confocal microscopy when the epithelium is leaky. This method not only obviate the installation of porous membrane to ease the fabrication but also allows local microscopic observation of cells at the point of adhesion over microchambers. In other words, it becomes possible to study the local barrier function depending on the location. By connecting these

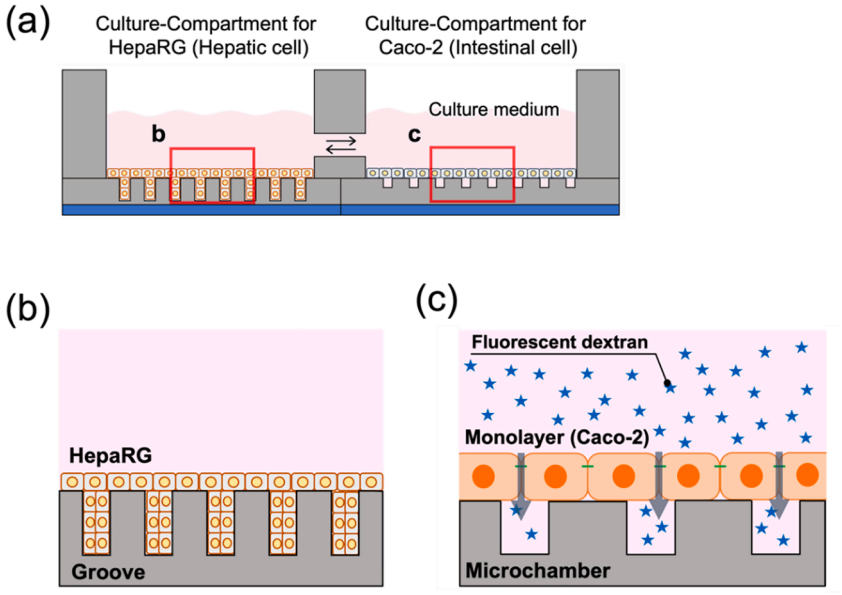

Fig. 1. (a) Schematic of the device cross-sectional view showing the microstructures and geometric distributions of liver (HepaRG) and intestinal (gut) (Caco-2) cells. (b) Liver cells cultured in microgrooves. (c) Intestinal cells cultured over microchambers. The paracellular permeability was evaluated by measuring the fluorescence intensity in microchambers emitted by the accumulated fluorescent marker molecules. All illustrations are drawn not to scale.

microstructured culture compartments with microchannels, we opted to examine the effect of HepaRG coculture over the permeability of Caco-2 monolayer.

3. Materials and methods

3.1. Fabrication

We designed and fabricated the co-culture device with two culture compartments as shown in Fig. 2(a) (see the picture of the actual device in the Supporting Information Fig. S1). The major dimensions of the device are shown in Fig. 2(b). The device is composed of the three layers of polydimethylsiloxane (PDMS) sheets and a cover glass bonded to the bottom. A top-layer includes the two culture compartments to contain the culture medium (Fig. 2(a-i)), while an intermediate layer contains a channel-network for metabolites transport between both compartments (Fig. 2(a-ii)). A thin bottom PDMS layer possesses microgrooves and microchambers dedicated to the 3D structuring of hepatocytes and permeability assay of intestinal monolayer, respectively (Fig. 2(a-iii)). Practically, high-aspect ratio series of grooves (width = 20 μm, 30 μm or 40 μm, depth = 40 μm) were engraved for the liver cells culture. For the permeability assay, a 5 × 5 array of 10 μm × 10 μm (10 μm deep) square microchambers is prepared as a unit array, and four regions of 256 (16 × 16) units were arranged in a single compartment (Fig. 2(c)). Columns of array units are numbered starting from the located at closest to the channel connected to the compartment for the hepatocyte culture as shown in the enlarged view.

The layer (i) was prepared by casting PDMS prepolymer (Silpot 184, DOW, USA) mixed with the curing agent at 10:1 wt ratio into a plastic dish to a height of 1 cm and then cured at 80 °C, 120 mins to produce PDMS slab. The PDMS slab was then cut and two holes with a diameter of 12.5 mm were opened using Cork borer. For layer (ii), PDMS prepolymer mixed with its curing agent was poured over the SU-8 mold of 80 connecting channels (height 80 μm, width 50 μm, and length 1000 μm) aligned in parallel to a thickness of approximately 1 mm. PDMS was then cured at 80 °C for 120 min. After demolding, adjacent holes of 12.5 mm diameter were made, taking care not to cut the connecting channels. The layer (iii) was obtained by spin-coating PDMS prepolymer with the curing agent over the Si mold of grooves or microchambers for 60 s. Spin-speeds 1000 rpm for grooves and 2000 rpm for microchambers, respectively, forming the layers having thicknesses of 50–80 μm and 30–60 μm. A cover glass was then placed over the coated PDMS and baked at 120 °C for 10 min to cure. Finally, by removing the cover glass from the mold after carefully cutting PDMS at sides, the PDMS layer (iii) with microstructures bonded to a cover glass was obtained (Supporting Information Fig. S2). Lastly, the fabricated layers (i)-(iii) were bonded after applying O_2 plasma for 10 s (PDC-32 G; Harrick Plasma, USA). Bonding process was done carefully to align the edges of the two cover glasses in layer (iii) with the space between the two holes in layer (ii) to prevent the medium from leaking out. This process allows formation of microstructures on the thin PDMS layer on a cover glass, enabling high-resolution imaging of cells cultured on in/on microstructures with a high-magnification objective lens.

3.2. Cell culture

HepaRG cell was provided by Biopredic International (France) and cultured following their provided guidelines. These cells were initially seeded at a density of 2×10^4 cells/cm^2 and maintained in William's E medium, which was supplemented with L-glutamine (2 mM), and the HepaRG® Growth Medium Supplement that contained antibiotics (ADD710, Biopredic International, France) (hereafter referred to as growth medium). The growth medium was refreshed every 2–3 days.

Caco-2 cell was supplied by American Type Culture Collection

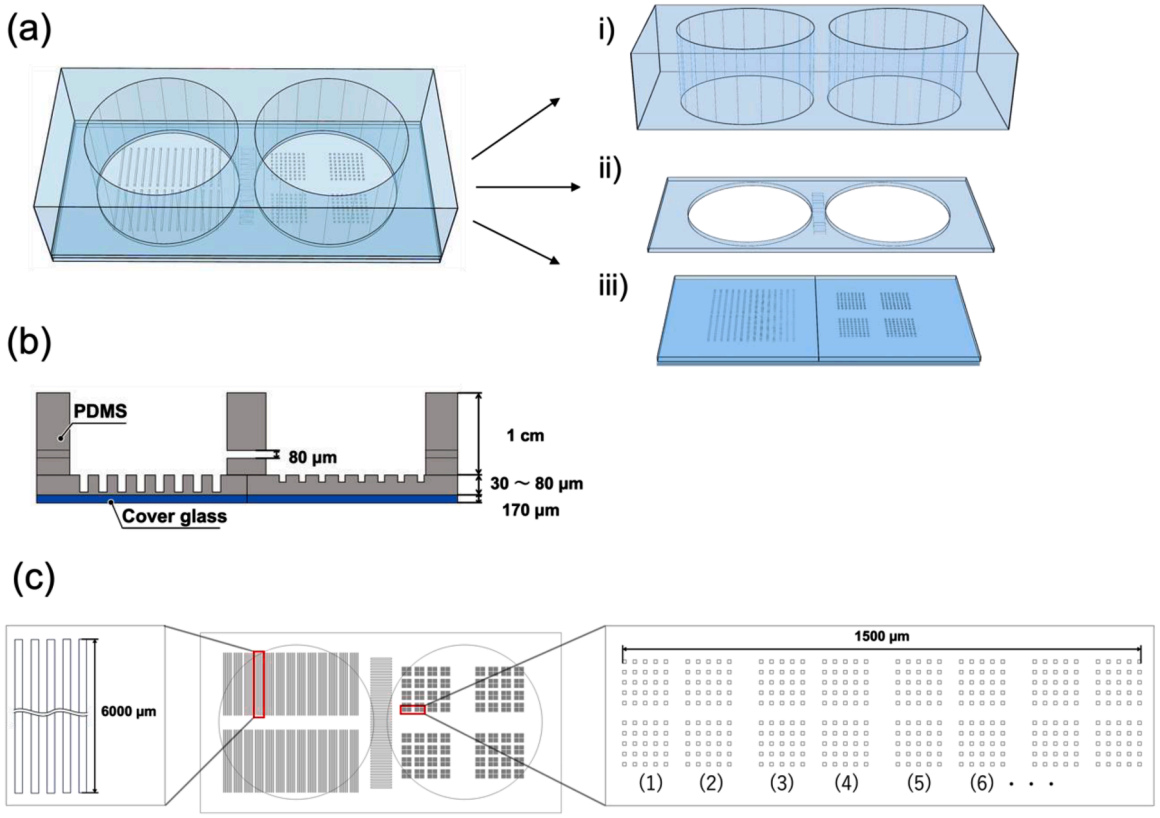

Fig. 2. (a) Schematic of the three-layered PDMS construction of the gut-liver co-culture MPS. (b) Cross-sectional view of the assembled co-culture device showing the major dimensions of the device. (c) Actual design of microstructures in the layer (iii). Local parts of the grooves and arrays of microchambers are enlarged on the left and right, respectively. Microchambers at different locations were used for the distance-dependent evaluation of the paracellular permeability.

(ATCC, France) and cultured according to their instructions. Cells were plated at a density of 4 × 10^4 cells/cm^2 and cultured with Dulbecco's Modified Eagle Medium (D-MEM) supplemented with 10% fetal bovine serum (FBS) and 1% penicillin/streptomycin (P/S). Passages were performed every 3–4 days. These two types of cells were incubated at 37 °C and 5% CO_2.

3.3. Cell culture in the device

In the co-culture device, PDMS surfaces of culture compartments for HepaRG and Caco-2 were coated with Collagen Type I from rat tail (SIGMA, USA) and Fibronectin from bovine plasma (SIGMA, USA), respectively. First, the device was sterilized by wrapping them in aluminum foil and heating them on a hot plate at 190 °C for 30 min. The device was then degassed in a vacuum chamber for 10 min, and a solution of Collagen Type I (50 μg/mL) was applied to the culture compartment with grooves immediately after removal from the vacuum chamber. Application of the 200 μL Collagen solution was enough to cover the surface within the compartment, and the solution was left for 30 min. Degassing the device prior to the application of coating solutions helped to remove air bubbles and to make the solution penetrate into microgrooves. Similarly, the culture compartment with microchambers was then coated with Fibronectin by applying 200 μL of Fibronectin solution (50 μg/mL) and left for 30 min. Lastly these solutions were removed by aspiration, and the device was washed twice with PBS.

After the coating of extracellular matrices, cells were seeded in compartments; HepaRG was adjusted to the density of 10,000 cells/500 μL and seeded in the culture compartment with grooves. Growth medium was used for 7 days from the day of cell seeding, and differentiation into hepatocytes was promoted by culturing cells in William's E medium, which was supplemented with HepaRG® differentiation medium supplement with antibiotics (ADD720, Biopredic International, France) containing 1.7% DMSO (hereafter referred to as differentiation medium) from the 8th day onward. Cultures were conducted for a total of 17 days (Fig. 3a). Meanwhile, Caco-2 was seeded at a density of 8,000 cells/500 μL and cultured with D-MEM for 17 days. The media were basically changed daily for both cells.

3.4. Permeability measurement

After establishing the Caco-2 cell monolayer, the culture medium was removed from the compartment, and the cells were rinsed with PBS. Subsequently, PBS solution containing fluorescent dextran (hereafter referred to as f-dextran; dextran conjugated with Fluorescein, 3,000 MW, anionic lysine fixable, D3305, Invitrogen, USA) was introduced into the compartment, and time-lapse recording within the microchambers commenced immediately using a confocal laser scanning microscope (Leica SP8 microscope with the objective Leica HCX PL Apo 40x/1.3 Oil, 11506329). As a control condition, we also performed the permeability assay without HepaRG. In this case, monoculture of Caco-2 was conducted in the culture compartment with microchambers, while only the media for HepaRG (up to day 7: growth medium, thereafter: differentiation medium) were added to the culture compartment with grooves (Fig. 3(b)).

A quantitative analysis of the captured images was then performed. Using an image analysis software (ImageJ, NIH), the fluorescent intensities within the microchambers in the time-lapse images were determined. Regions of interest (ROI), corresponding to the cross-sectional area of the microchambers, were defined, and the average intensities within these ROIs were recorded. The relative fluorescence intensity was calculated by dividing the temporal intensities within the microchambers by the average intensity within the microchambers when f-dextran was added in the absence of cells, serving as a reference.

3.5. Primary bile assay

Primary bile was derived from human sources and diluted to a given concentration in HepaRG differentiation medium and added to the culture compartment of HepaRG on day 7 or later of Caco-2 culture (Fig. 3(c)). Bile-containing HepaRG differentiation medium in the culture compartment with grooves was changed daily until day 17, when the permeability assay was performed.

3.6. Cell staining

To obtain the fluorescent images of live cells, Hoechst 33342

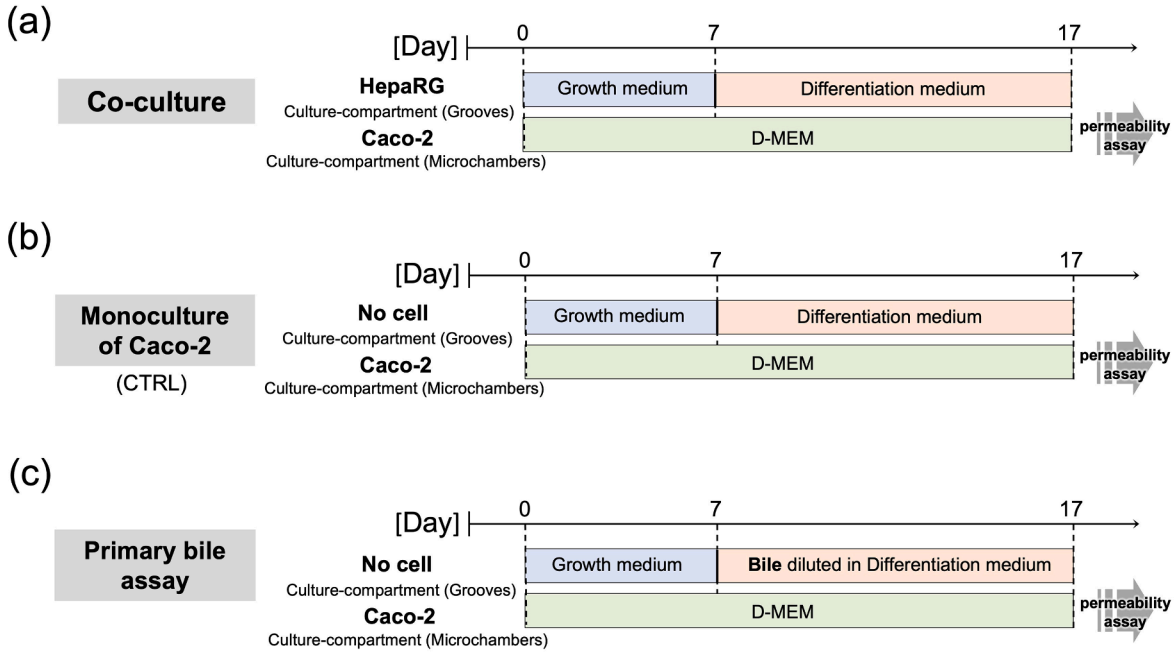

Fig. 3. Experimental schedule and types of media before the permeability assay of Caco-2 monolayer. (a) Co-culture of Caco-2 and HepaRG, (b) monoculture of Caco-2, and (c) monoculture of Caco-2 for the primary bile assay.

(H3570, Thermo Fischer Sci., USA) and 5-Carboxyfluorescein diacetate (5-CFDA, 79955–27–4, Abcam plc, UK) were used to stain the nuclei and bile canaliculi, respectively. For staining of Caco-2, each solution was prepared in medium (HepaRG: Differentiation medium, Caco-2: D-MEM) containing Hoechst 33342 at a concentration of 5 μg/mL and 5-CFDA at a concentration of 5 μg/mL. The entire cell culture medium was aspirated and the microdevice was rinsed once with PBS. A sufficient volume of the prepared solution (500 μL for one culture compartment) was added to completely cover the cell in the culture compartments. The microfluidic device with the solution was then placed in a CO_2 incubator for 30 min. Afterwards, the solutions were removed, cells were washed once with PBS, and observed by a confocal microscopy.

3.7. Statistical analysis

All the statistical analyses of the data were performed using GraphPad Prism 9 software (GraphPad, USA). Differences between 3 or more groups were analyzed using Kruskal-Wallis test with post hoc-Dunn's multiple comparison test.

4. Results

4.1. HepaRG differentiation in the microgrooves structure

Firstly, differentiation of HepaRG into hepatic tissues within micro grooves was evaluated. Practically, the formation of bile canaliculi by the hepatic tissues was investigated. We tested monocultures of HepaRG in several groove structures with different widths to evaluate the function of bile excretion. We used 5-Carboxyfluorescein diacetate (5-CFDA) marker that becomes fluorescent once hydrolyzed in the cytosol and excreted into the canaliculi by the specific transporters [26,33]. The adhesion pattern of HepaRG in grooves obtained by CLSM and their 3D reconstructed images are shown in Figs. S4 and 4, respectively. Green fluorescence of Carboxyfluorescein accumulated in canaliculi was observed with grooves having 20, 30, 40 μm width and 40 μm depth, confirming the differentiation of HepaRG into functional hepatocytes. The regions exhibiting green fluorescence tended to increase with increasing groove width. This result suggests that a wider groove width is more effective in promoting differentiation into hepatocyte tissue.

4.2. Culture and observation of Caco-2 using co-culture device

In our previous study, we showed that epithelial cells (Caco-2) cultured on microchambers formed a flat monolayer and that this structure can be used to evaluate the paracellular permeability [32]. The polarization of Caco-2 cultured over the microchamber was confirmed by immunostaining of ZO-1, a tight junction component protein. Here, we first tested whether a monolayer of Caco-2 is formed under the co-culture condition with HepaRG. Observation of Caco-2 at 17 days after the start of co-culture showed nuclei of Caco-2 stained with Hoechst 33342 were distributed on the flat surface of the microchamber device (Fig. 5(a)). Meanwhile, only a negligible fluorescence was observed when focusing on the plane inside microchambers (Fig. 5(b)), indicating that the culture condition necessary for the microchamber-based permeability assay of Caco-2 monolayer can be reproduced in the present experimental system. When f-dextran, as a marker of the paracellular permeability, was added to the cell supernatant typically after 7 days of culture, internal space within microchambers remained non-fluorescent, verifying the formation of tight paracellular barrier (Supporting Information Fig. S3 (a)). Occasionally, there were some places where the barrier was loose, and microchamber space fluoresced in such region (Supporting Information Fig. S3 (b,c)).

4.3. Caco-2 permeability assay in co-culture with HepaRG

Next, we evaluated differences in paracellular permeability between Caco-2 monocultures and those co-cultured with hepatocytes after 17 days culture. In the co-culture condition, experiments were performed with HepaRG cultured in 20, 30, and 40 μm grooves, respectively. The distributions of the intensity in microchambers at 120 min after addition of f-dextran show that permeation was significantly less in the co-culture condition compared to that in the monoculture condition (Fig. 6(a)). The intensity values under co-culture conditions showed that the paracellular permeation became more significant for wider groove widths, but it was similar for groove widths of 30 and 40 μm. This is expected to be due to the metabolites from HepaRG acting to decrease the permeability of Caco-2 under co-culture. We also consider that the decrease in intensity with 30 and 40 μm width compared to the groove width of 20 μm is due to the enhanced differentiation into hepatocyte tissue and the secretion of more metabolites such as bile as the groove width increased.

Next, taking advantage of the characteristics of our device, we locally analyzed fluorescence intensities from the array of microchambers

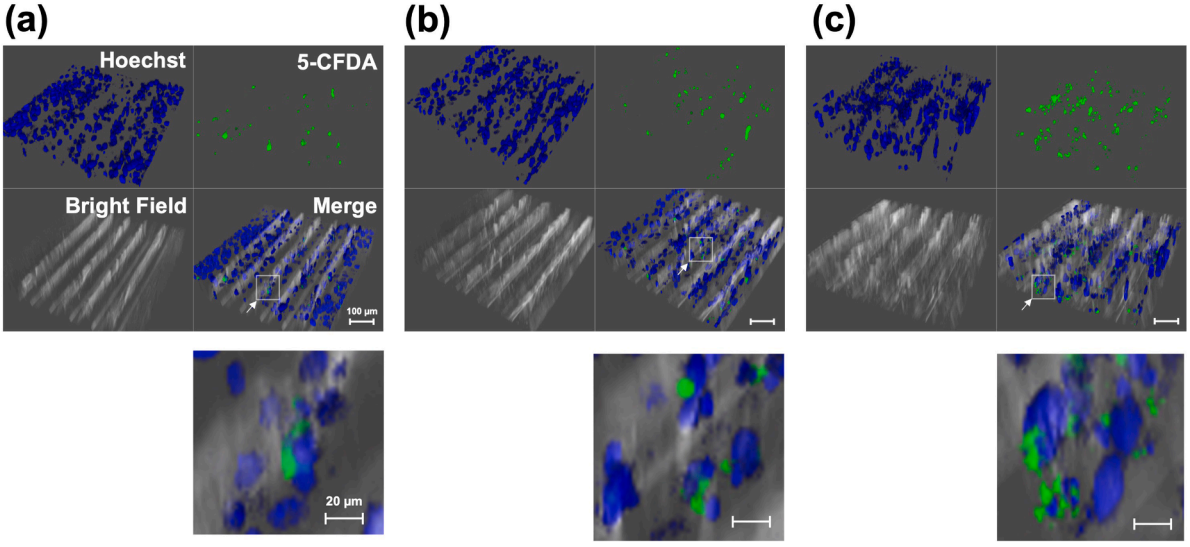

Fig. 4. Staining of bile canaliculi formed in HepaRG culture in grooves with (a) 20 μm (b) 30 μm (c) 40 μm widths. Nuclei stained by Hoechst 33342: blue, bile canaliculi stained by 5-CFDA: green. Enlarged views of the local spots, indicated by white rectangles, are shown in the bottom of each panel.

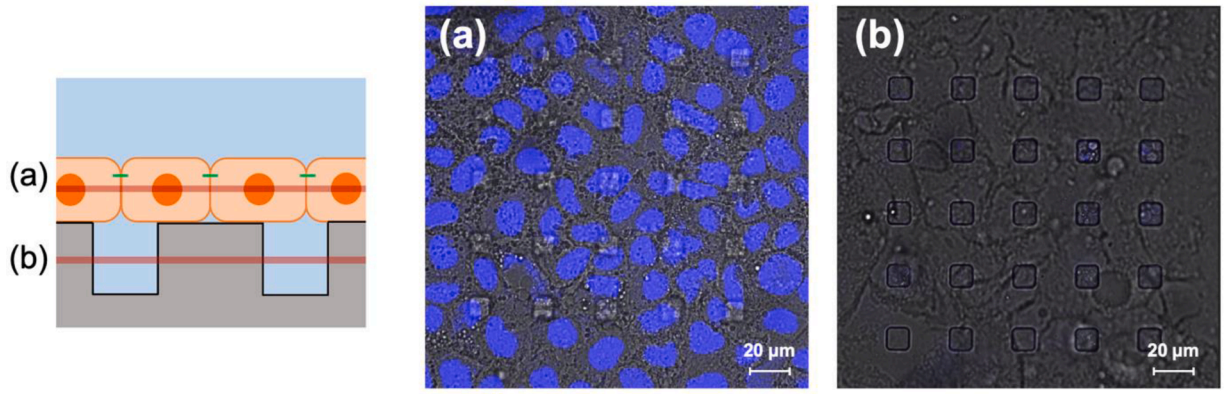

Fig. 5. Illustration depicting the cross-section of the cell sheet cultured over microchambers and actual planar images overlaying fluorescence and bright-field images. Focal planes of these images were set at (a) the cell monolayer on the device's surface and (b) inside the microchambers. Blue fluorescence represents nuclei stained by Hoechst.

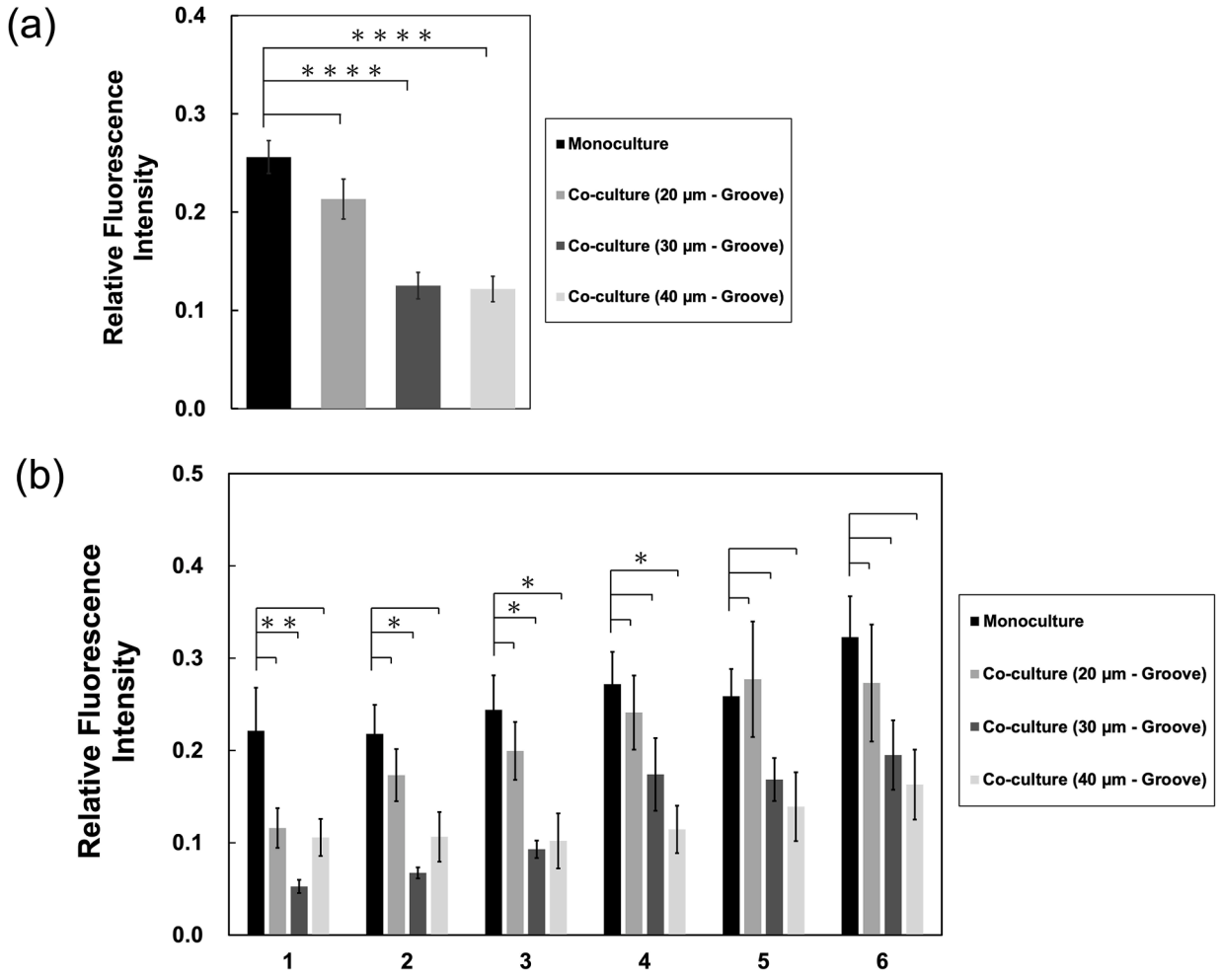

Fig. 6. Permeability assay of Caco-2 monolayer in the co-culture condition with HepaRG, which was cultured in grooves with different width. (a) Fluorescence intensities in microchambers at 120 min after the addition of f-dextran, relative to that in microchambers without Caco-2 cells. Averages and standard errors of 42 microchamber unites (six units in seven independent co-culture devices) are plotted. (b) The same relative intensities within each microchamber array at different locations (numbered from #1 to #6, Fig. 2c) in seven independent microdevices are plotted. Data are presented as mean ± SEM. Statistics performed by Kruskal-Wallis test, * $p < 0.05$, ** $p < 0.01$, **** $p < 0.0001$.

closest to the HepaRG culture compartment to the farthest from it (#1 to #6 in Fig. 2(c)). The fluorescence intensities in the microchambers at different locations obtained at 120 min after adding f-dextran, averaged across four devices, is shown Fig. 6(b). The results show that the fluorescence intensities during co-culture were lower in microchambers closer to the HepaRG culture compartment (closest one (#1) is located ~500 μm away from the end of the connecting channels) compared to that in the control (monoculture) experiment. This tendency was

particularly pronounced in the cases where grooves had widths of 30 or 40 μm, exhibiting significant differences from the control conditions. This result suggests that the concentration of the metabolites that diffused from HepaRG, increasing with the shorter distance, had stronger effect on the reduction of the permeability of Caco-2 cells when both types of cells are at a higher vicinity.

4.4. Permeability assay with the addition of primary bile

Finally, we tested the hypothesis that the cause of the decreased permeability of Caco-2 during co-culture with HepaRG could be the effect of bile secreted from HepaRG, a major metabolite of hepatocytes. We tested the response of Caco-2 by directly adding human primary bile into another compartment. In vivo, primary bile secreted by hepatocytes are transported to the intestine and metabolized by intestinal bacteria into secondary bile acids. Since the production of secondary bile acids by intestinal bacteria does not occur in our experimental system, we focused on primary bile and investigated their effects.

Practically, monoculture of Caco-2 was performed in the compartment with microchambers, while the medium, in which the bile was diluted along with differentiation medium, was exchanged daily in another compartment until day 17 (Fig. 3c). The results are shown in Fig. 7, showing the averages of fluorescence intensities in 24 microchamber units (six units in four independent co-culture devices) beneath Caco-2 monolayer at 120 min after addition of f-dextran. Bile at relatively high concentrations (100–500× dilution) tended to exhibit higher fluorescence intensity compared to the control experiment, while at lower concentrations (1000–10,000× dilution), the fluorescence intensity was slightly lower than that in the control experiment. Since the fluorescence intensity tended to be higher at high bile concentrations, it can be said that bile increased intestinal permeability in accordance with previously reports [27,34]. On the other hand, addition of the bile at low concentrations in turn tended to decrease intestinal permeability. In the significance test, significant difference was found only between the cases of the control (no bile) and 10,000× dilution, the lowest bile concentration. This result agrees with the result of co-culture experiment with HepaRG (Fig. 6). The lack of significant differences in higher concentrations of bile (100–500× dilution) was attributed to the high variability. Additionally, we locally analyzed fluorescence intensities from the array of microchambers closest to the HepaRG culture compartment to the farthest from it (Fig. S5; #1 to #6 in Fig. 2(c)). Although significant differences could not be observed at all locations except for #4, a trend of decreasing permeability (increasing barrier function) with decreasing bile concentration, which was augmented at the closer distances from the channel, was clearly observed. This analysis further supports our hypothesis.

5. Discussion

Bile acids, whose important components are cholic acid (CA), deoxycholic acid (DCA) and chenodeoxycholic acid (CDCA), are known to be cytotoxic, and their abnormal secretion has been shown to increase intestinal permeability by activating the epithelial growth factor receptor (EGFR) and following intracellular signaling pathway [27,29]. In a previous in vitro study, these bile acids at micromolar concentrations have been shown to increase intestinal paracellular permeability of Caco-2 (i.e., loosen the barrier function) [24]. Clinical results also show that bile acid secretion increases intestinal permeability [35]. The results of these studies provide an explanation for the significant increase of permeability observed at addition of high concentration of primary bile (Fig. 7).

On the other hand, the results of the co-culture with HepaRG, as well as those with additional bile at relatively low concentrations, exhibited decreased permeability (i.e., the barrier function was augmented). This seemingly contrary effect could be the result of complexity in the components and their concentrations in bile and other secreted materials, which regulates the integrity of intestinal barrier [28,36]. Since the bile secreted from HepaRG is known to have the most in vivo like bile acid profile [37], it is likely that this observed decrease in permeability in both experiments is caused by a similar mechanism. Previously, Kimura et al. [38] reported that co-culture of intestinal cells (hiPS) and primary hepatocytes (PXB cells) resulted in an increase in the TEER value of intestinal cells (e.g., augmented barrier function), accompanied by a predominant increase in the expression level of occludin, a tight junction component protein [39,40] although, no discussion of the specific metabolite responsible for this change was provided. Furthermore, in 1995, Hashimoto et al. [41] reported the augmentation of the barrier function of intestinal Caco-2-SF cell, which do not have stable tight junction, upon addition of milk whey proteins. They determined the β-lactoglobulin (β-LG) and bovine serum albumin (BSA) in whey is responsible for this change. Additionally, Song et al. [42] reported that tauroursodeoxycholic acid (TUDCA) improves the intestinal barrier function, although this scenario is unlikely to applicable in the present study because TUDCA is a component in secondary bile acids after microbial transformation. Since albumin is abundant in secretions from hepatocytes in including bile [43], the scenario in Ref. [41] could be responsible for the observed decrease in intestinal permeability at co-culture and dilute bile assays, although detailed analysis will be

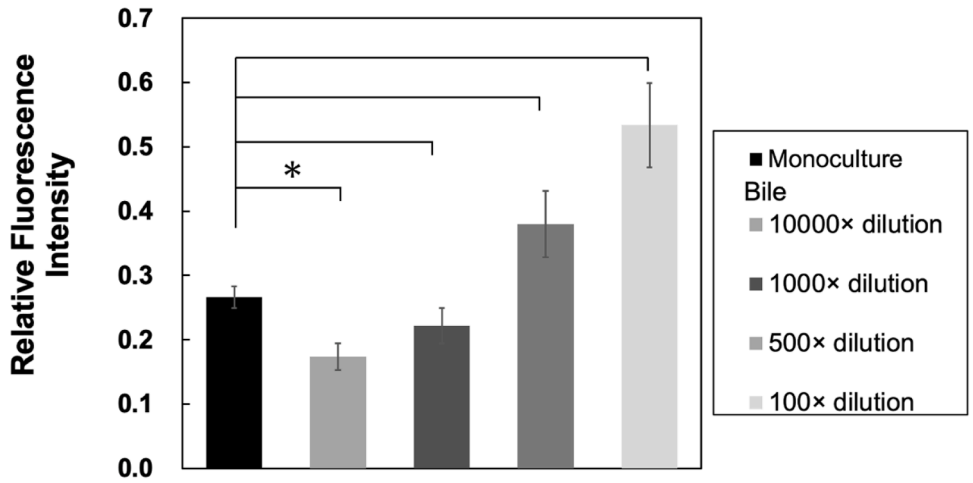

Fig. 7. Relative fluorescence intensities in microchambers measured at 120 min after the addition of f-dextran with or without primary bile at different concentrations introduced in another compartment. Averages and standard errors of 24 microchamber units (six units in four independent co-culture devices) are plotted. Statistics performed by Kruskal-Wallis test, * $p < 0.05$.

necessary to identify the responsible players. Nonetheless, the organ-to-organ interactions are intrinsically complex, and we can conclude that our simple co-culture device would help recapitulating liver-gut interactions.

6. Conclusion

We have developed and evaluated a microdevice that enables the co-culturing of hepatic cells and intestinal epithelial cells for testing their functional interactions. This device consists of two culture compartments, comprising microgrooves for hepatocyte culture and microchambers for the epithelial permeability assay. This approach eliminates the need for external fluidic pumps and tubings during cell cultivation and simplifies the manufacturing process significantly by not requiring electrodes or porous membranes for the assessment of intestinal epithelial barrier function.

Here, we conducted co-culture of HepaRG and Caco-2 as a liver-gut axis model. Especially, use of HepaRG highlighted the possible effects of bile. Using 5-CFDA, we confirmed the promotion of bile canaliculus formation with the widening of the grooves and consequently a better hepatic cell differentiation. We compared the permeability of Caco-2 monolayer between the monoculture and the co-culture with HepaRG cells. It became evident that the permeability of Caco-2 cells decreased when co-cultured with HepaRG cells. The interaction between hepatocytes and intestinal cells is quite complex, and the effects of bile are still unresolved. Future studies are needed to investigate how bile metabolized from cells and other substances affect the permeability of intestinal cells, and our device could provide an effective means.

To summarize, we described the open system to simplify co-culture of cells from two organs to see their interactions. There is a prospect of transitioning this system to realize a perfusion condition to better mimic in vivo conditions. Under perfusion conditions, co-culture of intestinal epithelial cells with gut bacteria has been reported [44]. The intestinal tract and gut bacteria are closely related, and it is known that the metabolism of primary bile acids into secondary bile acids occurs by the action of gut bacteria [28]. Such a perusable flow system could be an important perspective for simulating the physiological environment more accurately. In conclusion, our simple microdevice revealed that co-culturing with HepaRG cells appears to impact the permeability of Caco-2 monolayer, with bile being a potential influencing factor.

CRediT authorship contribution statement

Ryuya Kida: Writing – review & editing, Writing – original draft, Visualization, Methodology, Investigation, Formal analysis, Data curation, Conceptualization. **Alan Rajendran:** . **Mamiko Tsugane:** Writing – review & editing, Writing – original draft, Funding acquisition, Formal analysis, Data curation, Conceptualization. **Jean-Charles Duclos-Vallée:** Writing – review & editing, Methodology. **Maxime M Mahe:** . **Sakina Bensalem:** Writing – review & editing, Investigation, Conceptualization. **Hiroaki Suzuki:** Writing – review & editing, Writing – original draft, Supervision, Project administration, Funding acquisition, Conceptualization. **Bruno Le Pioufle:** Writing – review & editing, Writing – original draft, Supervision, Resources, Project administration, Methodology, Conceptualization.

Declaration of competing interest

The authors declare that they have no known competing financial interests or personal relationships that could have appeared to influence the work reported in this paper.

Data availability

No data was used for the research described in the article.

Acknowledgments

This study was supported by JSPS Grant-in-Aids (19H05626), Shimadzu Science Foundation, Japan Keirin Autorace foundation (JKA), and the Institute of Science and Engineering at the Chuo University. The authors also acknowledge the support from the french Agence Nationale de la Recherche (Dili-on-Chip ANR 21-CE19-0025 project). The study was performed using the technical platforms of Institut d'Alembert CNRS FR3242, ENS Paris-Saclay.

References

[1] S. Fowler, W. Li, K. Chen, D.B. Duignan, A. Gupta, N. Hariparsad, J.R. Kenny, W. G. Lai, J. Liras, J.A. Phillips, J. Gan, Microphysiological systems for ADME-related applications: current status and recommendations for system development and characterization, Lab Chip 20 (2020) 446–467, https://doi.org/10.1039/c9lc00857h.

[2] D.E. Ingber, Human organs-on-chips for disease modelling, drug development and personalized medicine, Nat. Rev. Genet. 23 (2022) 467–491, https://doi.org/10.1038/s41576-022-00466-9.

[3] A.K. Kopec, R. Yokokawa, N. Khan, I. Horii, J.E. Finley, C.P. Bono, C. Donovan, J. Roy, J. Harney, A.D. Burdick, B. Jessen, S. Lu, M. Collinge, R.B. Sadeghian, M. Derzi, L. Tomlinson, J.E. Burkhardt, Microphysiological systems in early stage drug development: perspectives on current applications and future impact, J. Toxicol. Sci. 46 (2021) 99–114, https://doi.org/10.2131/jts.46.99.

[4] J. Seok, H. Shaw Warren, G.C. Alex, N.M. Michael, V.B. Henry, W. Xu, D. R. Richards, G.P. McDonald-Smith, H. Gao, L. Hennessy, C.C. Finnerty, C.M. López, S. Honari, E.E. Moore, J.P. Minei, J. Cuschieri, P.E. Bankey, J.L. Johnson, J. Sperry, A.B. Nathens, T.R. Billiar, M.A. West, M.G. Jeschke, M.B. Klein, R.L. Gamelli, N. S. Gibran, B.H. Brownstein, C. Miller-Graziano, S.E. Calvano, P.H. Mason, J. P. Cobb, L.G. Rahme, S.F. Lowry, R.V. Maier, L.L. Moldawer, D.N. Herndon, R. W. Davis, W. Xiao, R.G. Tompkins, Genomic responses in mouse models poorly mimic human inflammatory diseases, Proc. Natl. Acad. Sci. U. S. A. 110 (2013) 3507–3512, https://doi.org/10.1073/PNAS.1222878110.

[5] R. Franco, A. Cedazo-Minguez, Successful therapies for Alzheimer's disease: why so many in animal models and none in humans? Front. Pharmacol. 146 (5) (2014) https://doi.org/10.3389/fphar.2014.00146.

[6] K. Fabre, B. Berridge, W.R. Proctor, S. Ralston, Y. Will, S.W. Baran, G. Yoder, T. R. Van Vleet, Introduction to a manuscript series on the characterization and use of microphysiological systems (MPS) in pharmaceutical safety and ADME applications, Lab Chip 20 (2020) 1049–1057, https://doi.org/10.1039/C9LC01168D.

[7] M. Agrawal, S. Kumar Deshmukh, D. Gurbani, Y. Teng, C. Jensen, Is it time to start transitioning from 2D to 3D cell culture? Front. Mol. Biosci. 33 (7) (2020) https://doi.org/10.3389/fmolb.2020.00033.

[8] D. Huh, B.D. Matthews, A. Mammoto, M. Montoya-Zavala, H. Yuan Hsin, D. E. Ingber, Reconstituting organ-level lung functions on a chip, Science 328 (2010) 1662–1668, https://doi.org/10.1126/science.1188302.

[9] M. Abulaiti, Y. Yalikun, K. Murata, A. Sato, M.M. Sami, Y. Sasaki, Y. Fujiwara, K. Minatoya, Y. Shiba, Y. Tanaka, H. Masumoto, Establishment of a heart-on-a-chip microdevice based on human iPS cells for the evaluation of human heart tissue function, Sci. Rep. 19201 (10) (2020), https://doi.org/10.1038/s41598-020-76062-w.

[10] A. Bein, W. Shin, S. Jalili-Firoozinezhad, M.H. Park, A. Sontheimer-Phelps, A. Tovaglieri, A. Chalkiadaki, H.J. Kim, D.E. Ingber, H. John, A. Paulson, Microfluidic organ-on-a-chip models of human intestine, Cell. Mol. Gastroenterol. Hepatol. 5 (4) (2018) 659–668, https://doi.org/10.1016/j.jcmgh.2017.12.010.

[11] L. Ewart, A. Apostolou, S.A. Briggs, C.V. Carman, J.T. Chaff, A.R. Heng, S. Jadalannagari, J. Janardhanan, K.J. Jang, S.R. Joshipura, M.M. Kadam, M. Kanellias, V.J. Kujala, G. Kulkarni, C.Y. Le, C. Lucchesi, D.V. Manatakis, K. K. Maniar, M.E. Quinn, J.S. Ravan, A.C. Rizos, J.F.K. Sauld, J.D. Sliz, W. Tien-Street, D.R. Trinidad, J. Velez, M. Wendell, O. Irrechukwu, P.K. Mahalingaiah, D. E. Ingber, J.W. Scannell, D. Levner, Performance assessment and economic analysis of a human liver-chip for predictive toxicology, Commun. Med. 154 (2) (2022), https://doi.org/10.1038/s43856-022-00209-1.

[12] B. Peng, S. Hao, Z. Tong, H. Bai, S. Pan, K.L. Lim, L. Li, N.H. Voelcker, W. Huang, Blood–brain barrier (BBB)-on-a-chip: a promising breakthrough in brain disease research, Lab Chip 22 (2022) 3579–3602, https://doi.org/10.1039/D2LC00305H.

[13] S.R. Moses, J.J. Adorno, A.F. Palmer, J.W. Song, Vessel-on-a-chip models for studying microvascular physiology, transport, and function *in vitro*, Am. J. Physiol. Cell Physiol. 320 (2020) 92–105, https://doi.org/10.1152/ajpcell.00355.2020.

[14] A. Albillos, A. de Gottardi, M. Rescigno, The gut-liver axis in liver disease: pathophysiological basis for therapy, J. Hepatol. 72 (2020) 558–577, https://doi.org/10.1016/j.jhep.2019.10.003.

[15] S. Anand, S.S. Mande, Host-microbiome interactions: gut-Liver axis and its connection with other organs, NPJ Biofilms Microbiomes 89 (8) (2022), https://doi.org/10.1038/s41522-022-00352-6.

[16] M. Meroni, E. Paolini, M. Longo, R. Piciotti, G. Tria, S. Fargion, A.L. Fracanzani, P. Dongiovanni, Recreating gut-liver axis during NAFLD onset by using a Caco-2/HepG2 co-culture system, Metab. Target Organ Damage 2 (4) (2022), https://doi.org/10.20517/mtod.2021.19.

[17] C. Ge, X. Huang, S. Zhang, M. Yuan, Z. Tan, C. Xu, Q. Jie, J. Zhang, J. Zou, Y. Zhu, D. Feng, Y. Zhang, J. Aa, *In vitro* co-culture systems of hepatic and intestinal cells for cellular pharmacokinetic and pharmacodynamic studies of capecitabine against colorectal cancer, Cancer Cell Int. 23 (14) (2023), https://doi.org/10.1186/s12935-023-02853-6.

[18] N. Milani, N. Parrott, D. Ortiz Franyuti, P. Godoy, A. Galetin, M. Gertz, S. Fowler, Application of a gut–liver-on-a-chip device and mechanistic modelling to the quantitative in vitro pharmacokinetic study of mycophenolate mofetil, Lab Chip 22 (2022) 2853–2868, https://doi.org/10.1039/D2LC00276K.

[19] N. Tsamandouras, W.L.K. Chen, C.D. Edington, C.L. Stokes, L.G. Griffith, M. Cirit, Integrated gut and liver microphysiological systems for quantitative in vitro pharmacokinetic studies, AAPS J. 19 (2017) 1499–1512, https://doi.org/10.1208/s12248-017-0122-4.

[20] J. Yang, Y. Hirai, K. Iida, S. Ito, M. Trumm, S. Terada, R. Sakai, T. Tsuchiya, O. Tabata, K. Kamei, Integrated-gut-liver-on-a-chip platform as an in vitro human model of non-alcoholic fatty liver disease, Commun. Biol. 6 (310) (2023) 310, https://doi.org/10.1038/s42003-023-04710-8.

[21] H. Kimura, T. Ikeda, H. Nakayama, Y. Sakai, T. Fujii, An on-chip small intestine–liver model for pharmacokinetic studies, J. Lab Autom. 20 (2015) 265–273, https://doi.org/10.1177/2211068214557812.

[22] M. Shinohara, H. Arakawa, Y. Oda, N. Shiraki, S. Sugiura, T. Nishiuchi, T. Satoh, K. Iino, S. Leo, Y. Kato, K. Araya, T. Kawanishi, T. Nakatsuji, M. Mitsuta, K. Inamura, T. Goto, K. Shinha, W. Nihei, K. Komori, M. Nishikawa, S. Kume, Y. Kato, T. Kanamori, Y. Sakai, H. Kimura, Coculture with hiPS-derived intestinal cells enhanced human hepatocyte functions in a pneumatic-pressure-driven two-organ microphysiological system, Sci. Rep. 11 (2021) 5437, https://doi.org/10.1038/s41598-021-84861-y.

[23] S.G. Kang, Y.Y. Choi, S. Mo, T.H. Kim, J.H. Ha, D.K. Hong, H. Lee, S.D. Park, J. J. Shim, J.L. Lee, B.G. Chung, Effect of gut microbiome-derived metabolites and extracellular vesicles on hepatocyte functions in a gut-liver axis chip, Nano Converg. 10 (2023) 5, https://doi.org/10.1186/s40580-022-00350-6.

[24] B. Srinivasan, A.R. Kolli, M.B. Esch, H.E. Abaci, M.L. Shuler, J.J. Hickman, TEER measurement techniques for *in vitro* barrier model systems, J. Lab. Autom. 20 (2015) 107–126, https://doi.org/10.1177/2211068214561025.

[25] D.H. Elbrecht, C.J. Long, J.J. Hickman, Transepithelial/endothelial electrical resistance (TEER) theory and ap-plications for microfluidic body-on-a-chip devices, J. Rare Dis. Res. Treat. 1 (2016) 46–52, https://doi.org/10.29245/2572-9411/2016/3.1026.

[26] M. Boul, N. Benzoubir, A. Messina, R. Ghasemi, I.B. Mosbah, J.C. Duclos-Vallée, A. Dubart-Kupperschmitt, B.L. Pioufle, A versatile microfluidic tool for the 3D culture of HepaRG cells seeded at various stages of differentiation, Sci. Rep. 11 (2021) 14075, https://doi.org/10.1038/s41598-021-92011-7.

[27] F. Raimondi, P. Santoro, M.V. Barone, S. Pappacoda, M.L. Barretta, M. Nanayakkara, C. Apicella, L. Capasso, R. Paludetto, Bile acids modulate tight junction structure and barrier function of Caco-2 monolayers via EGFR activation, Am. J. Physiol. Gastrointest. Liver Physiol. 294 (2008) 906–913, https://doi.org/10.1152/AJPGI.00043.2007.

[28] N. Calzadilla, S.M. Comiskey, P.K. Dudeja, S. Saksena, R.K. Gill, W.A. Alrefai, Bile acids as inflammatory mediators and modulators of intestinal permeability, Front. Immunol. 13 (2022) 1021924, https://doi.org/10.3389/fimmu.2022.1021924.

[29] L. Shi, L. Jin, W. Huang, Bile acids, intestinal barrier dysfunction, and related diseases, Cells 12 (14) (2023) 1888, https://doi.org/10.3390/cells12141888.

[30] B. Delalat, C. Cozzi, S. Rasi Ghaemi, G. Polito, F.H. Kriel, T.D. Michl, F.J. Harding, C. Priest, G. Barillaro, N.H. Voelcker, Microengineered Bioartificial liver chip for drug toxicity screening, Adv. Funct. Mater. 28 (2018) 1801825, https://doi.org/10.1002/ADFM.201801825.

[31] M. Tsugane, E. Uejima, H. Suzuki, Microchamber device for detection of transporter activity of adherent cells, Front. Bioeng. Biotechnol. 3 (32) (2015), https://doi.org/10.3389/fbioe.2015.00032.

[32] R. Kida, M. Tsugane, H. Suzuki, Horizontal and vertical microchamber platforms for evaluation of the paracellular permeability of an epithelial cell monolayer, Lab Chip (2024), https://doi.org/10.1039/D3LC00855J.

[33] H. Suemizu, K. Nakamura, K. Kawai, Y. Higuchi, M. Kasahara, J. Fujimoto, A. Tanoue, M. Nakamura, Hepatocytes buried in the cirrhotic livers of patients with biliary atresia proliferate and function in the livers of urokinase-type plasminogen activator-NOG mice, Liver Transpl. 20 (2014) 1127–1137, https://doi.org/10.1002/lt.23916.

[34] A. Fasano, G. Budillon, S. Guandalini, R. Cuomo, G. Parrilli, A.M. Cangiotti, M. Morroni, A. Rubino, Bile acids reversible effects on small intestinal permeability, Digest. Dis. Sci. 35 (1990) 801–808, https://doi.org/10.1007/BF01536791.

[35] R. Cabrera-Rubio, A.M. Patterson, P.D. Cotter, N. Beraza, Cholestasis induced by bile duct ligation promotes changes in the intestinal microbiome in mice, Sci. Rep. 9 (2019) 12324, https://doi.org/10.1038/s41598-019-48784-z.

[36] A.L. Ticho, P. Malhotra, P.K. Dudeja, R.K. Gill, W.A. Alrefai, Bile acid receptors and gastrointestinal functions, Liver Res. 3 (2019) 31–39, https://doi.org/10.1016/j.livres.2019.01.001.

[37] V.M.P. De Bruijn, Z. Wang, W. Bakker, W. Zheng, B. Spee, H. Bouwmeester, Hepatic bile acid synthesis and secretion: comparison of in vitro methods, Toxicol. Lett. 365 (2022) 46–60, https://doi.org/10.1016/j.toxlet.2022.06.004.

[38] K. Shinha, W. Nihei, H. Nakamura, T. Goto, T. Kawanishi, N. Ishida, N. Yamazaki, Y. Imakura, S. Mima, K. Inamura, H. Arakawa, M. Nishikawa, Y. Kato, Y. Sakai, H. Kimura, A kinetic pump integrated microfluidic plate (Kim-plate) with high usability for cell culture-based multiorgan microphysiological systems, Micromachines 12 (9) (2021), https://doi.org/10.3390/mi12091007 (Basel).

[39] O.R. Colegio, C. Van Itallie, C. Rahner, J.M. Anderson, Claudin extracellular domains determine paracellular charge selectivity and resistance but not tight junction fibril architecture, Am. J. Physiol. Cell Physiol. 284 (2003) 1346–1354, https://doi.org/10.1152/AJPCELL.00547.2002.

[40] R. Al-Sadi, K. Khatib, S. Guo, D. Ye, M. Youssef, T. Ma, Occludin regulates macromolecule flux across the intestinal epithelial tight junction barrier, Am. J. Physiol. Gastrointest. Liver Physiol. 300 (2011) 1054–1064, https://doi.org/10.1152/AJPGI.00055.2011.

[41] K. Hashimoto, K. Takeda, T. Nakayama, M. Shimizu, Stabilization of the tight junction of the intestinal caco-2 cell monolayer by milk whey proteins, Biosci. Biotechnol. Biochem. 59 (1995) 1951–1952, https://doi.org/10.1271/bbb.59.1951.

[42] M. Song, F. Zhang, Y. Fu, X. Yi, S. Feng, Z. Liu, D. Deng, Q. Yang, M. Yu, C. Zhu, X. Zhu, L. Wang, P. Gao, G. Shu, X. Ma, Q. Jiang, S. Wang, Tauroursodeoxycholic acid (TUDCA) improves intestinal barrier function associated with TGR5-MLCK pathway and the alteration of serum metabolites and gut bacteria in weaned piglets, J. Anim. Sci. Biotechnol. 73 (13) (2022), https://doi.org/10.1186/s40104-022-00713-3.

[43] J.L. Boyer, Bile formation and secretion, Compr. Physiol. 3 (3) (2013) 1035–1078, https://doi.org/10.1002/cphy.c120027.

[44] H.J. Kim, D. Huh, G. Hamilton, D.E. Ingber, Human gut-on-a-chip inhabited by microbial flora that experiences intestinal peristalsis-like motions and flow, Lab Chip 12 (2012) 2165–2174, https://doi.org/10.1039/c2lc40074j.